THE JOURNAL OF BIOLOGICAL CHEMISTRY

Vol. 267, No. 8, Issue of March 15, pp. 5217-5221, 1992
Printed in U.S.A.

Purification, Characterization, and Nucleotide Sequence of the Thermolabile α-Amylase from the Antarctic Psychrotroph *Alteromonas haloplanctis* A23*

(Received for publication, September 23, 1991)

Georges Feller‡, Thierry Lonhienne, Christophe Deroanne, Cecille Libioulle, Jozef Van Beeumen§, and Charles Gerday

From the Laboratory of Biochemistry, Institute of Chemistry B6, University of Liege, B-4000 Liege, Belgium and the §Laboratory of Microbiology, University of Gent, B-9000 Gent, Belgium

The α-amylase excreted by the antarctic bacterium *Alteromonas haloplanctis* was purified and the corresponding *amy* gene was cloned and sequenced. N- and C-terminal amino acid sequencing were used to establish the primary structure of the mature *A. haloplanctis* α-amylase which is composed of 453 amino acids with a predicted M_r of 49,340 and a pI of 5.5. Three Ca^{2+} ions are bound per molecule and its activity is modulated by chloride ions. Within the four consensus sequences, Asp-174, Glu-200, and Asp-264 are the proposed catalytic residues. The psychrotrophic *A. haloplanctis* α-amylase is characterized by a high amylolytic activity at low temperatures, a reduced apparent optimal temperature, and typical thermodynamic activation parameters. *A. haloplanctis* α-amylase has also a low thermal stability as demonstrated by the temperature effect on both activity and secondary structure. It is suggested that structure flexibility and lower sensitivity of secondary structure to temperature variations in the low temperature range are the main structural adaptations of the psychrotrophic enzyme. The unusual stacking of small amino acids around the catalytic residues is proposed as a factor inducing active site flexibility and concomitant high activity of the enzyme at low temperatures.

The properties of proteins from extremophilic bacteria are commonly used to gain further insights in the structure-function and structure-stability relationships of enzymes (1). Whereas analysis of thermophilic strains are well documented, enzymes from psychrotrophic bacteria have received little attention (2) and most functional traits of enzymes adapted to low temperatures have been gained from ectothermic invertebrates and vertebrates. As a rule, these cold-adapted enzymes are characterized by high k_{cat} and physiological efficiency (K_{cat}/K_m) as well as by a low and rather constant K_m at temperatures close to that of their natural environment. These enzymes display an apparent optimal activity shifted towards low temperatures and manifest pronounced heat lability (3, 4).

These properties confer to cold-active enzymes a great economical value since enzymatically driven reactions can be carried out within a temperature range of 0–20 °C at which homologous mesophilic enzymes have their catalytic activity drastically reduced (5). One can also take advantage of the heat lability of these enzymes for selectively inactivating them in a complex medium as already proposed for an antarctic bacterial alkaline phosphatase (6).

The study of the structural and catalytic parameters of these cold-active proteins is still fragmental and the molecular basis of protein adaptation to cold remains unknown (4, 7). The adaptations of psychrotrophic enzymes to catalysis at low temperatures are not simply the opposite phenomenon of thermophilic enzymes. The latter are faced with the problem of stability at high temperatures, whereas the former have essentially to cope with the reduction of the enzymatic reaction rates near 0 °C in order to maintain adequate metabolic fluxes. A detailed analysis of the properties and structures of some psychrotrophic enzymes will certainly contribute to a better understanding of protein folding and protein dynamics.

In this context, we have selected an antarctic *bacterium* excreting α-amylase (α-1,4-glucan-4-glucanohydrolase, EC 3.2.1.1). This model enzyme was chosen because α-amylases from several organisms have been characterized and sequenced (8–10). The conserved amino acid residues involved in substrate binding, Ca^{2+} binding, and in the catalytic process have been assessed by site-directed mutagenesis and x-ray diffraction studies (11, 12). In addition, the refined three-dimensional structure of porcine pancreatic α-amylase and of two *Aspergillus* α-amylases are available (12–14).

Here we report the characterization of the *A. haloplanctis* α-amylase with special emphasis on the effects of temperature on the activity and stability of this enzyme. The primary structure of the psychrotrophic α-amylase deduced from the nucleotide sequence and partial amino acid sequencing is also discussed in relation to the adaptational strategy of enzymes to low temperatures.

EXPERIMENTAL PROCEDURES AND RESULTS[1]

* This work was supported by Fonds de la Recherche Fondamentale Collective Research Contract 2.4526.92 and the Belgium National program on Fundamental Research in Life Sciences, Science Policy Programming Department, Contract BIO 22. The costs of publication of this article were defrayed in part by the payment of page charges. This article must therefore be hereby marked "*advertisement*" in accordance with 18 U.S.C. Section 1734 solely to indicate this fact.

The nucleotide sequence(s) reported in this paper has been submitted to the GenBank™/EMBL Data Bank with accession number(s) X58627.

‡ To whom correspondence should be addressed.

[1] Portions of this paper (including "Experimental Procedures," "Results," Figs. 1–6, and Tables I and II) are presented in miniprint at the end of this paper. The abbreviations used are: AHA, *A. haloplanctis* α-amylase; BAA, *B. amyloliquefaciens* α-amylase; Et-G_7-PNP, ethylidene-*p*-nitrophenyl maltoheptaoside; Hepes, *N*-2-hydroxyethylpiperazine-*N'*2-ethanesulfonic acid; MES, 2-(*N*-morpholino)ethanesulfonic acid; PAGE, polyacrylamide gel electrophoresis; SDS, sodium dodecyl sulfate. Miniprint is easily read with the aid of a standard magnifying glass. Full size photocopies are included in the microfilm edition of the Journal that is available from Waverly Press.

DISCUSSION

The α-amylase excreted by the bacterium *A. haloplanctis* share most of its structural properties with other microbial α-amylases (*i.e.* molecular weight, isoelectric point, amino acid composition, ion requirements). Alignment of the four conserved regions with those of α-amylases of known three-dimensional structure (12–14) allows to locate the functional amino acids. The catalytic pair of aspartic acids of *A. haloplanctis* α-amylase would be Asp-174 and Asp-264, with Glu-200 acting in substrate binding. The primary Ca^{2+}-binding site essential in maintaining proper folding around the active site would involve the conserved Asn-88 and His-178. Beside water molecules, Asn-136 and Asp-144 are two other potential ligands. The secondary Ca^{2+}-binding site would implicate Asp-174 and Glu-200. Finally, comparison with porcine pancreatic amylase indicates that Arg-172, Lys-224, and Lys-300 would be the chloride ligands of *A. haloplanctis* α-amylase

The enzyme is thus suitable for the analysis of molecular adaptations required to compensate for the reduction of enzyme activity inherent to low temperatures. In order to maintain adequate amylolytic activity for its metabolism, the antarctic strain synthetizes a catalyst characterized by high k_{cat} and physiological efficiency (k_{cat}/K_m) as well as by a lower E_a. Since such differences in the kinetic behavior have also been noted when comparing enzymes from ectothermic and endothermic species (28), the psychrotrophic *A. haloplanctis* α-

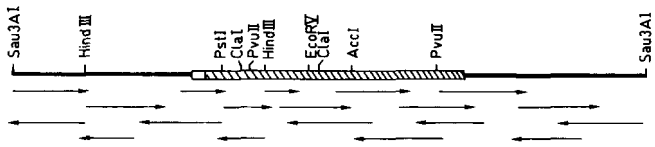


```
                                                                    GATCAAATTCAGAAAATTGCATAGAGTGTCTAAAATAAGGGACAATTACCCTGATTATCGCGCTATGCTGCGCTTGGTGAATGAAAAGG
90  TGAAAAAATGTCTGGTTTTGTATTTAAACAATTTAAAGTTGAACACGACCACTGTGCAATGAAAGTTTCTACCGATGGCATTTTGCTTGGCGCATGGGCTAATTTAAGCGGTGCAAAGTCATT
213 ACTTGATATAGGCACCGGCACCGGCTTACTAGCACTAATGTGTAAGCAGCGCAGTAGTGAGCTTGATATAACTGCGGTAGAAATTGACGAAAGCGCCTATACCCAACCATTACAAAATGTAGC
336 TAATAGCCCGTGGCCAACAATAAGTATTACGCATCAAACTATTCAAGCTTTAGTAGTGAAGTTAAATTTGACGTGGTTATCTCTAATCCACCGTATTTTAATCACAGTTTAAAAGGCGATAAT
459 GTTGCGCGTAATACCGCACGCCATACCGACGGCCTAAGTTTTGAAGAGTTAATTAATGCGTTTAAACATTTAAGCCATAGAGGTTCTCGCTTTAGCTTAATACTCCCAAGCATTGAAGGCGCA
582 TTATTTATTGAGCTTGCTACTCAAAATGGGCTTTATTTAAATACTCACTGCCAAGTAAAAGCCACGCCCAATAAAGATATTAGCCGCAGTTTAATGACATTTAGCTACGTAAAAAGCGATATA
705 GAAACATCAATTCTGTGTATTAGAAACTTAGATAATACCTACACTGCTGATTATATAGCCCTGTGCAAAGCATTTTATTTGAAAATGTAAATTGCCTAGTTATGTAGGTTATCTAGTAATAAA
828 GGATAATTTACCTATTATGCATACGTATTCAGTTTTTATTTAATCAATTACCAATCTAGTGTTAACCACTTGTAAATAACATCGAGTAGTTGTTTTGCTCGCTCAACAATTGGATCACACACT
                                                                                                -35          -10          SD
-24 Met Lys Leu Asn Lys Ile Ile Thr Thr Ala Gly Leu Ser Leu Gly Leu Leu Leu Pro Ser Ile Ala Thr Ala Thr Pro Thr Thr Phe Val His
951 ATG AAA CTC AAT AAA ATA ATC ACC ACC GCA GGT TTA AGC CTA GGG TTG CTC TTA CCT AGC ATT GCG ACT GCT ACG CCC ACC ACA TTT GTA CAT

8   Leu Phe Glu Trp Asn Trp Gln Asp Val Ala Gln Glu Cys Glu Gln Tyr Leu Gly Pro Lys Gly Tyr Ala Ala Val Gln Val Ser Pro Pro Asn
1044 TTG TTT GAA TGG AAT TGG CAA GAT GTA GCG CAA GAA TGT GAG CAA TAC CTA GGA CCA AAA GGC TAC GCT GCA GTA CAG GTC TCG CCA CCT AAT

39  Glu His Ile Thr Gly Ser Gln Trp Trp Thr Arg Tyr Gln Pro Val Ser Tyr Glu Leu Gln Ser Arg Gly Gly Asn Arg Ala Gln Phe Ile Asp
1137 GAG CAC ATT ACA GGA AGC CAA TGG TGG ACA CGT TAT CAG CCA GTA AGT TAT GAA CTG CAA AGT CGT GGC GGA AAC CGT GCA CAG TTT ATC GAT

70  Met Val Asn Arg Cys Ser Ala Ala Gly Val Asp Ile Tyr Val Asp Thr Leu Ile Asn His Met Ala Ala Gly Ser Gly Thr Gly Thr Ala Gly
1230 ATG GTA AAT CGC TGT AGT GCA GCT GGG GTT GAT ATT TAC GTT GAT ACG CTT ATT AAC CAT ATG GCA GCA GGA AGT GGC ACA GGC ACG GCG GGA

101 Asn Ser Phe Gly Asn Lys Ser Phe Pro Ile Tyr Ser Pro Gln Asp Phe His Glu Ser Cys Thr Ile Asn Asn Ser Asp Tyr Gly Asn Asp Arg
1323 AAT AGC TTT GGT AAT AAA AGC TTT CCT ATT TAT AGC CCA CAA GAT TTT CAT GAA AGT TGT ACC ATT AAT AAC TCT GAT TAT GGC AAC GAT CGC

132 Tyr Arg Val Gln Asn Cys Glu Leu Val Gly Leu Ala Asp Leu Asp Thr Ala Ser Asn Tyr Val Gln Asn Thr Ile Ala Ala Tyr Ile Asn Asp
1416 TAC CGA GTA CAA AAC TGT GAA CTA GTT GGA CTT GCC GAT TTA GAT ACC GCT TCA AAC TAT GTG CAA AAT ACC ATT GCA GCA TAT ATT AAC GAC

163 Leu Gln Ala Ile Gly Val Lys Gly Phe Arg Phe Asp Ala Ser Lys His Val Ala Ala Ser Asp Ile Gln Ser Leu Met Ala Lys Val Asn Gly
1509 TTA CAA GCT ATT GGC GTA AAA GGC TTT CGG TTT GAT GCT TCT AAA CAT GTT GCA GCA AGC GAT ATC CAA AGT TTA ATG GCC AAA GTA AAT GGC

194 Ser Pro Val Val Phe Gln Glu Val Ile Asp Gln Gly Gly Glu Ala Val Gly Ala Ser Glu Tyr Leu Ser Thr Gly Leu Val Thr Glu Phe Lys
1602 TCG CCA GTG GTT TTT CAA GAA GTG ATC GAT CAA GGT GGG GAG GCT GTT GGT GCC TCT GAA TAT TTA AGC ACA GGT TTA GTA ACT GAA TTT AAA

225 Tyr Ser Thr Glu Leu Gly Asn Thr Phe Arg Asn Gly Ser Leu Ala Trp Leu Ser Asn Phe Gly Glu Gly Trp Gly Phe Met Pro Ser Ser Ser
1695 TAT AGC ACT GAG CTT GGT AAC ACT TTT AGA AAC GGC TCG CTT GCA TGG CTG AGT AAT TTT GGC GAA GGG TGG GGC TTT ATG CCA AGC TCT TCT

256 Ala Val Val Phe Val Asp Asn His Asp Asn Gln Arg Gly His Gly Gly Ala Gly Asn Val Ile Thr Phe Glu Asp Gly Arg Leu Tyr Asp Leu
1788 GCG GTG GTT TTT GTA GAC AAT CAC GAC AAT CAG CGC GGG CAC GGC GGC GCT GGC AAT GTT ATT ACC TTT GAA GAT GGC CGC TTA TAT GAC TTA

287 Ala Asn Val Phe Met Leu Ala Tyr Pro Tyr Gly Tyr Pro Lys Val Met Ser Ser Tyr Asp Phe His Gly Asp Thr Asp Ala Gly Gly Pro Asn
1881 GCC AAT GTA TTT ATG TTG GCT TAT CCG TAC GGT TAT CCA AAA GTA ATG TCG AGT TAT GAT TTT CAT GGT GAT ACA GAT GCT GGT GGG CCA AAT

318 Val Pro Val His Asn Asn Gly Asn Leu Glu Cys Phe Ala Ser Asn Trp Lys Cys Glu His Arg Trp Ser Tyr Ile Ala Gly Gly Val Asp Phe
1974 GTA CCG GTA CAT AAT AAT GGT AAC TTA GAG TGT TTT GCG AGT AAT TGG AAG TGT GAG CAT CGC TGG TCA TAT ATT GCA GGC GGG GTC GAT TTT

349 Arg Asn Asn Thr Ala Asp Asn Trp Ala Val Thr Asn Trp Trp Asp Asn Thr Asn Asn Gln Ile Ser Phe Gly Arg Gly Ser Ser Gly His Met
2067 AGA AAT AAC ACC GCC GAC AAC TGG GCA GTA ACA AAT TGG TGG GAT AAC ACA AAT AAT CAA ATT TCA TTT GGC CGA GGT AGC TCG GGT CAT ATG

380 Ala Ile Asn Lys Glu Asp Ser Thr Leu Thr Ala Thr Val Gln Thr Asp Met Ala Ser Gly Gln Tyr Cys Asn Val Leu Lys Gly Glu Leu Ser
2160 GCT ATT AAC AAA GAA GAC TCA ACA CTT ACT GCA ACT GTG CAA ACC GAT ATG GCG TCA GGG CAA TAC TGT AAT GTG CTA AAA GGC GAA CTG TCA

411 Ala Asp Ala Lys Ser Cys Ser Gly Glu Val Ile Thr Val Asn Ser Asp Gly Thr Ile Asn Leu Asn Ile Gly Ala Trp Asp Ala Met Ala Ile
2253 GCT GAT GCT AAA AGT TGT AGT GGT GAG GTT ATA ACG GTT AAT TCC GAC GGT ACT ATT AAT CTT AAT ATT GGC GCT TGG GAT GCG ATG GCA ATT

442 His Lys Asn Ala Lys Leu Asn Thr Ser Ser Ala Ser ***
2346 CAT AAA AAT GCC AAG TTA AAT ACC AGT TCT GCC TCA TAGCACTGAAAGTGACTGGCAGCGAACGGTTATTTTTATTAATGCACAAACACAAAGCGGACAAGATATGTTTAT

2457 CCGTGGTGGAATTGACCACGCTTATGCAAACGCAAACCTTGGTCGAAATTGCCAAACAAGTAATTTTGAGTGTGCAATGCCTATTCGTCATAACAATTTAAAAAATGTCACAACAAGCCCTTG
2580 GAAAGCAAATGATAACTACCTTGATTGGTATGGTATAGAAAATGGGCAAAGTAGCGAACGAGAAGGTTCTGCTACGACTGGACAACGAACGTTTGGCCAGCAGGTTGGGGCGCTGAAAAAACG
2703 GTAAACACAGATGGTTTTGGTGTGACACCTTTAAATATATGGGGCGAACACTATTGGATGCTTGATGTAGATATGGATTGCAGTAAAGCGGTTAATGGATGGTTTGAACTAAAAGCATTCATT
2826 AAAAATGGCCAAGGATGGGAGACTGCCATTGCACAAGACAATGCACCTTATACAAGTACTAATCATATGGCGCAATGCGGAAAAATTAATAAATTTGAGTTTAATAATTCAGGTGTAGTAATT
2949 CGTAGTTTTTAAAAGTAAGCAAAAAAGCTCATATGAAAACCTAAACTAATGATTATTAGTTTAGGTTTTTTGCTTATGTACAGCGCTTTAATAGTGTGTGTTTATAAATCACCTGATATGATT
3072 TAGCCATTGGCCACTTAATTTAAAAGGCAATACAATGAAAAGTTAAATAAATTAGCATTACTTAGCAGCTTAGCAGCCACCATTTTTGCAAGCCAAGGTGTGTTTGCTGCTATTACGCCTGT
3195 AGGGCTTTGGAAAACAATTGATGAGGATACAAACCAAGCTAAGTCGTATGTACGTATTACCCAAACCAGCGGTGTATTGAGCGGCAAAGTTGAAACCATTCTTAACCCGGCAAAACAAAATGA
3318 TATATGTAGTAAATGCGATGATGAGTTAAAAGATC
```

FIG. 7. **Nucleotide sequence of the *amy* gene from *A. haloplanctis* A23.** *Upper panel:* physical map showing some restriction endonuclease cleavage sites and α-amylase coding region (*dashed box*). The sequencing strategy is indicated, *arrows* showing direction and extend of sequencing. *Lower panel:* nucleotide sequence and predicted primary structure of the α-amylase precursor. Amino acids are numbered starting at the signal peptidase cleavage site. The cleavage site is located by a *vertical bar*. The potential promoter regions (−35, −10), the Shine-Dalgarno sequence (*SD*), the stop codon (***), and the inverted repeats (*arrows*) are indicated. Amino acids confirmed by N- and C-terminal sequencing are *underlined*. The four conserved peptides are *boxed*.

amylase displays an extreme trend of the cold adaptation characters.

The simplest view of the enzyme adaptations to catalysis at low temperatures is to postulate that the psychrotrophic enzyme possesses a more flexible structure in order to undergo rapid and reversible conformation modifications required by the catalytic cycle. If this is true, both psychrotrophic and mesophilic enzymes should have roughly the same conformation in the physiological range of temperature of the parent organism. This seems indeed illustrated by the CD spectra (Fig. 5) in which one can observe that $[\Theta]_{222}$ of both enzymes reaches identical values at 5 °C for *A. haloplanctis* α-amylase and around 40 °C for *Bacillus amyloliquefaciens* α-amylase. In addition, an improved structure flexibility would also explain how the cold-adapted enzyme takes advantage of the thermodynamic characteristics of its environment to ensure the formation of the enzyme-substrate activated complex. The enthalpic and entropic contribution to ΔG^* (Table II) agree with the fact that a more flexible enzyme structure would reach an activated conformation with less heat content and that the increase in free energy corresponding to the activated complex will be reached through a minimum of entropy change.

The loose conformation of the psychrotrophic enzyme implies a reduction of its structural stability which is well reflected by the increased denaturing effect of urea as well as by the thermostability curves, the shift of the optimal temperature of activity, and the fast disorganization of the secondary structures indicated by CD spectra. The ellipticity values (Fig. 5) also suggest that the folding of *A. haloplanctis* α-amylase is less affected by temperature variations in the low temperature range; concomitantly, its amylolytic activity is also less dependent of temperature (lower E_a or Q_{10}) than *B. amyloliquefaciens* α-amylase in that range. It is worth mentioning that this property in conjunction with the above mentioned protein flexibility can account for all the observed structural and kinetic characteristics of the antarctic enzyme.

By analogy with thermophilic enzymes which seem to rely on hydrophobic interactions to improve the internal packing arrangement of the protein (1), one would expect a reduction of these weak bonds in psychrotrophic enzymes. This is not reflected by the relative content of hydrophobic amino acid residues of *A. haloplanctis* α-amylase nor by its hydropathy profile. However, assuming that urea acts mainly by weakening hydrophobic bonds, the sensitivity of *A. haloplanctis* α-amylase to urea could indeed reflect a decrease of this type of bonds. Enhancement of thermostability has been observed by introduction of a disulfide bond in subtilisin (29). Accordingly, lowering disulfide linkage in *A. haloplanctis* α-amylase would be another way to increase the flexibility of the peptide backbone. This possibility is, however, ruled out by the lack of cysteine residue in most *Bacillus* α-amylases. On the other hand, we have previously suggested that the stacking of Gly around the catalytic residues of three psychrotrophic lipases could provide high active site flexibility (30). Interestingly, *A. haloplanctis* α-amylase also display an unusual concentration of Gly, Ala, and Ser on both sides of the conserved catalytic peptides. Such a concentration of small-sized amino acids, which could provide regions of chain flexibility (31), is not found in any other microbial or vertebrate α-amylase. Finally, the reduced thermal sensitivity of the secondary structures of *A. haloplanctis* α-amylase before denaturation can be achieved by a delicate balance between weak bounds of opposite enthalpy of formation. Confirmation of these hypothesis requires the knowledge of the three-dimensional structure of the enzyme.

Acknowledgments—The Expeditions Polaires Françaises are acknowledged for the support and facilities offered at the Antarctic station Dumont d'Urville. We thank J. Swings (University of Gent) for identification of the antarctic strain and N. Gerardin-Otthiers, S. Collin, and R. Marchand for expert technical assistance.

REFERENCES

1. Mozhaev, V. V., Berezin, I. V., and Martinek, K. (1988) *CRC Crit. Rev. Biochem.* **23,** 235–281
2. Morita, R. Y. (1975) *Bacteriol. Rev.* **39,** 144–167
3. Somero, G. N. (1977) *J. Exp. Zool.* **194,** 175–188
4. Hochachka, P. W., and Somero, G. N. (1984) *Biochemical Adaptations*, Princeton University Press, Princeton, NJ
5. Dambmann, C., and Aunstrup, K. (1981) in *Proteinases and Their Inhibitors: Structure, Function, and Applied Aspects* (Turk, V., and Vitale, L., eds) pp. 231–244, Pergamon Press, Oxford
6. Kobori, H., Sullivan, C. W., and Shizuya, H. (1984) *Proc. Natl. Acad. Sci. U. S. A.* **81,** 6691–6695
7. Jaenicke, R. (1990) *Phil. Trans. R. Soc. Lond. B* **326,** 535–553
8. Vihinen, M., and Mäntsälä, P. (1989) *Crit. Rev. Biochem. Mol. Biol.* **24,** 329–418
9. Svensson, B. (1988) *FEBS Lett.* **230,** 72–76
10. Raimbaud, E., Buleon, A., Perez, S., and Henrissart, B. (1989) *Int. J. Biol. Macromol.* **11,** 217–225
11. Vihinen, M., Ollikka, P., Niskanen, J., Meyer, P., Suominen, I., Karp, M., Holm, L., Knowles, J., and Mäntsälä, P. (1990) *J. Biochem.* (*Tokyo*) **107,** 267–272
12. Boel, E., Brady, L., Brzozowski, A. M., Derewenda, Z., Dodson, D. D., Jensen, V. J., Petersen, S. B., Swift, H., Thim, L., and Woldike, H. F. (1990) *Biochemistry* **29,** 6244–6249
13. Matsuura, Y., Kusunoki, M., Harada, W., and Kakudo, M. (1984) *J. Biochem.* (*Tokyo*) **95,** 697–702
14. Buisson, G., Duée, E., Haser, R., and Payan, F. (1987) *EMBO J.* **6,** 3909–3916
15. Biely, P., Mislovicova, D., Markovic, O., and Kalac, V. (1988) *Anal. Biochem.* **172,** 176–179
16. Chung, H., and Friedberg, F. (1980) *Biochem. J.* **185,** 387–395
17. Rauscher, E., Neumann, U., Schaich, E., von Bülow, S., and Wahlefeld, A. W. (1985) *Clin. Chem.* **31,** 14–19
18. Bernfeld, P. (1955) *Methods Enzymol.* **1,** 149–151
19. Takkinen, K., Pettersson, R. F., Kalkkinen, N., Palva, I., Söderlund, H., and Kääriäinen, L. (1983) *J. Biol. Chem.* **258,** 1007–1013
20. Chen, Y. H., Yang, J. T., and Martinez, H. M. (1972) *Biochemistry* **11,** 4120–4131
21. Feller, G., Thiry, M., Arpigny, J. L., and Gerday, Ch. (1991) *Gene* (*Amst.*) **102,** 111–115
22. Feller, G., Thiry, M., Arpigny, J. L., Mergeay, M., and Gerday, Ch. (1990) *FEMS Microbiol. Lett.* **66,** 239–244
23. Ogasahara, K., Imanishi, A., and Isemura, T. (1970) *J. Biochem.* (*Tokyo*) **67,** 65–75
24. Hasegawa, A., Miwa, N., Oshima, T., and Imahori, K. (1976) *J. Biochem.* (*Tokyo*) **79,** 35–42
25. Staden, R. (1984) *Nucleic Acids Res.* **12,** 505–519
26. von Heijne, G. (1985) *J. Mol. Biol.* **184,** 99–105
27. Watson, M. (1984) *Nucleic Acids Res.* **12,** 5145–5164
28. Low, P. S., Bada, J. L., and Somero, G. N. (1973) *Proc. Natl. Acad. Sci. U. S. A.* **70,** 430–432
29. Takagi, H., Takahashi, T., Momose, H., Inouye, M., Maeda, Y., Matsuzawa, H., and Ohta, T. (1990) *J. Biol. Chem.* **265,** 6874–6878
30. Feller, G., Thiry, M., and Gerday, Ch. (1991) *DNA Cell Biol.* **10,** 381–388
31. Karplus, P. A., and Schulz, G. E. (1985) *Naturwissenschaften* **72,** 212–213

Continued on next page.

Supplemental Material to
PURIFICATION, CHARACTERIZATION AND NUCLEOTIDE SEQUENCE OF THE THERMOLABILE α-AMYLASE FROM THE ANTARCTIC PSYCHROTROPH *Alteromonas haloplanctis* A23

Georges Feller, Thierry Lonhienne, Christophe Deroanne, Cécille Libioulle, Jozef Van Beeumen, and Charles Gerday

EXPERIMENTAL PROCEDURES

Sources- The heterotrophic aerobic strain *Alteromonas haloplanctis* A23 was isolated from sea water at the Dumont d'Urville antarctic station (60°40' S; 40°01' E). Selection for amylolytic activity was carried out on Marine agar 2216E (Difco) containing 0.1% OBR-amidon synthetized as described (15). The α-amylase from *Bacillus amyloliquefaciens* (16) was from Sigma (A6380).

Purification of AHA- The antarctic strain was cultivated at 4°C for 3 days in 3.5 l of broth containing 10 g/l bactotryptone, 5 g/l yeast extract, 33 g/l NaCl, 40 g/l maltose, pH 7.6, vigorously aerated by air bubbling. Addition of maltose was found to induce α-amylase excretion in the supernatant by 3-fold. After centrifugation at 11,000 g, the culture supernatant was made 0.02% NaN_3, then concentrated up to 400 ml and diafiltrated against 50 mM Tris-HCl, 1 mM $CaCl_2$, pH 7.5 using a Minitan tangential flow ultrafiltration unit (Millipore) fitted with PTGC membranes (10,000 nmwl). The sample was then loaded on a DEAE-agarose column (2.5 x 40 cm) equilibrated in the above mentioned buffer and eluted with a NaCl linear gradient (500ml-500ml, 1 M NaCl buffer). Fractions containing amylolytic activity were concentrated to 10 ml and applied on a Sephacryl S-200 column (2.5 x 100 cm) eluted with 50 mM Tris-HCl, 1 mM $CaCl_2$, pH 7.0 followed by gel filtration on an Ultrogel AcA 54 column (2.5 x 100 cm) eluted with the same buffer. For further experiments, the purified AHA was conditioned in the appropriate buffers by gel filtration on PD10 column (Pharmacia) or lyophilyzed in 25 mM NH_4HCO_3.

Enzyme assay- Standard assay was carried out with the α-amylase EPS kit (Boehringer) using 3 mM Et-G_7-PNP as substrate and excess (23 U/ml) of a-glucosidase (EC 3.2.1.20) as coupling enzyme in 100 mM Hepes, 50 mM NaCl, 10 mM $MgCl_2$, pH 7.1 (17). Activities towards the synthetic substrate were recorded in a thermostated Uvicon 860 spectrophotometer (Kontron) and calculated on the basis of an extinction coefficient for Et-G_7-PNP of 8,650 $M^{-1}cm^{-1}$ at 405 nm. The effects of pH, ions and urea on the amylolytic activity were determined by the dinitrosalicylic acid method (18) using 1% soluble starch (Sigma) as substrate. In all experiments the pH was kept constant at the various temperatures.

Analytical procedures- The energy of activation (Ea) was determined from the slope (-Ea/R) of Arrhenius plots and the thermodynamic activation parameters of the amylolytic reaction were calculated according to the following equations :

$\Delta G^* = \Delta H^* - T\Delta S^*$

$\Delta H^* = Ea - RT$

$\Delta S^* = 2.303\ R\ (\log k_{cat} - 10.753 - \log T + Ea/2.303\ RT)$

Amino acid analyses were performed on native and carboxymethylated proteins hydrolysed for 24, 48 and 72 h using a Dionex DC300 amino acid analyser, equipped with a Waters dual wavelength colorimeter model 440 and a HPLC polystyrene sulfonic column (Waters, 0.4 x 25 cm). Concentration of the purified α-amylases was determined by amino acid analysis of the samples used.

Isoelectric focusing and polyacrylamide gel electrophoresis in presence of SDS or in non denaturing continuous conditions were run essentially as described by the supplier of the electrophoresis equipment (Hoeffer Scientific Instruments).

Calcium bound to AHA was measured using a Perkin Elmer 303 atomic absorption spectrophotometer, after dialysis of the enzyme solutions against 2x250 ml of high purity water at 4°C. The last dialysis solution was taken as a blank.

Circular dichroism spectra of protein dissolved in 25 mM phosphate buffer (pH 7.0) were recorded in a 0.1 cm path length cell under constant nitrogen flush using a thermostated dichrograph Jobin-Yvon Mark V. Data were expressed in terms of the mean residue ellipticity Θ. The mean residue weight of the mature proteins was calculated from the amino acid composition deduced from the nucleotide sequence. Sequence of *B. amyloliquefaciens* α-amylase (BAA) was taken from (19). The α helix content of the enzymes was estimated according to the following equations (20) where

$\Theta_{222} = \Delta\varepsilon \times 3300$ and $f\alpha = (\Theta_{222} + 2{,}340)/-30{,}300$

The NH_2-terminal amino acid sequence of the native AHA was determined using a pulsed liquid phase protein sequencer Applied Biosystems 477A equipped with on-line 120A PTH analyser and also a PI 2090E enhanced integrated micro-sequencing system including a PTH micro-analyser module (Porton Instruments). The COOH-terminal amino acid analysis was carried out on 10 nmol purified AHA dissolved in 200 µl of 100 mM pyridine acetate buffer, 1% SDS, 0.1 mM norleucine, pH 5.7, digested with 0.1 nmol carboxypeptidase Y (Sigma). Following acidification by 5 µl acetic acid and freeze drying of timed aliquots, the liberated amino acids were analysed as described above.

Cloning and sequencing- Genomic DNA of *A. haloplanctis* was partially digested with *Sau*3AI and the resulting fragments were inserted into the single *Bam*HI site of pSP73 (Promega).The ligated DNA was electroporated in *E.coli* RR1 cells and the transformants were selected on L-agar plates containing 100 µg ampicillin/ml and 1% soluble starch. The temperature of growth and incubation was controlled as previously described (21). The AHA gene-containing DNA fragment was subcloned into the polylinker of the phagemid pGEM 3Z f+ and f- (Promega). Single strand DNA was obtained by infecting pGEM 3Zf transformed *E.coli* JM109 cells with the helper phage M13K07, inducing the bacteriophage f1 replication (pGEM Single Strand System, Promega). The sequence was determined by the dideoxynucleotide chain termination method using Sequenase (US Biochemical Corp.). Synthetic oligonucleotides complementary to the plasmid sequences and internal sequences (provided by Eurogentec SA) were used as primers.

RESULTS

Effect of temperature on α-amylase excretion- The antarctic strain *Alteromonas haloplanctis* is able to grow from 0°C to about 25°C and is therefore referred to as a psychrotrophic bacterium (2). However, temperatures higher than that normaly experienced by the bacterium (-2° to 4°C) have pronounced effect on AHA excretion : in comparison with cultures run at 4°C, the maximal amylolytic activity recorded in supernatants is only 13% at 18°C and 6% at 25°C. This effect of temperature on enzyme excretion is similar to that reported for antarctic *Moraxella* strains producing exolipases (22).

Characterization of the psychrotrophic α-amylase- The purification protocol described under the Materials and Methods section allowed us to obtain AHA in a fairly pure state as judged by gel electrophoresis in denaturing or non denaturing conditions as well as by isoelectric focusing (Fig. 1). This procedure lead to a 250-fold purification factor with about 60 % yield. The apparent molecular weight of the purified AHA has been estimated to be 50,000 and its isoelectric point to be pH 5.5. The calculated extinction coefficient was $\varepsilon_{280} = 56.2\ 10^3\ M^{-1}cm^{-1}$. Calcium assay determined by atomic absorption indicated that AHA is a metalloprotein containing 3 Ca^{2+} per mole of enzyme. The optimum pH value for activity and stability of the psychrotrophic AHA has been found near neutrality as shown in Fig. 2a.

Chloride ions are essential for activity of the psychrotrophic α-amylase. Desalting AHA and BAA in 50 mM Hepes-NaOH, pH 7.0 on a Sephadex PD 10 column results in the complete loss of activity in the case of the antarctic α-amylase. Addition of NaCl, but not Na_2SO_4, restores the amylolytic activity and a dissociation constant of about 3 mM was calculated from the saturation curve (not shown). The psychrotrophic AHA is also more urea-sensitive than BAA (Fig. 2b). Addition of 3 M urea in the reaction medium induces 80 and 60 % inhibition of the activity of AHA and BAA respectively.

Thermal stability- The denaturation curves of both the psychrotrophic and the mesophilic enzymes were recorded in various conditions (Fig. 3). The results can be summarized as follows : i) contrarily to the α-amylases from the *Bacillus* species, no stabilizing effect of Ca^{2+} was found for AHA; ii) chloride concentrations up to 0.5 M strongly stabilize AHA but not BAA; iii) even in optimal conditions, AHA is less stable than its mesophilic counterpart, a common character of cold-adapted enzymes (4).

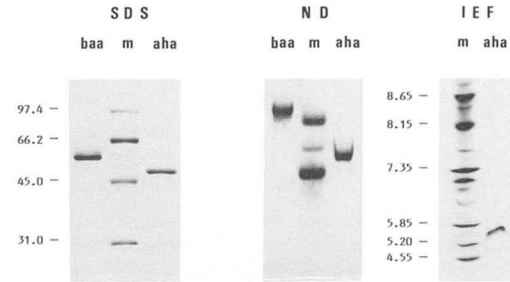

Fig. 1 : Polyacrylamide gel electrophoresis of the purified AHA. AHA and BAA were analyzed by SDS-PAGE (SDS), non denaturing PAGE (ND) and isoelectric focusing (IEF). The following marker proteins (M) were used : SDS; phosphorylase b (97.4 kDa), bovine serum albumin (66.2 kDa), ovalbumin (45 kDa) and carbonic anhydrase (31 kDa). ND; carp parvalbumins 2, 3 and 4a. IEF; lentil lectin (pH 8.65 and pH 8.15), horse myoglobin (pH 7.35), bovine carbonic anhydrase (pH 5.85), β lactoglobulin A (pH 5.20), soybean trypsin inhibitor (pH 4.55).

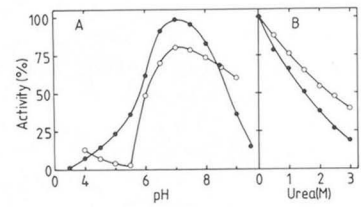

Fig. 2 : Determination of pH optima (A) and effect of urea (B) on AHA.
A : effect of pH on activity (●) and stability (○) of AHA. The buffers used were 25 mM acetate NaOH, 20 mM NaCl between pH 3.5 - pH 5.5 and 25 mM MES, 25 mM Hepes, 25 mM Tris, 20 mM NaCl between pH 5.5 - pH 9.5. Activities were recorded at 25°C using 1 % starch as substrate in these buffers. Residual activities were recorded after 24 h incubation at 5°C in these buffers using Et-G_7-PNP as substrate.
B : effect of urea in the reaction medium of AHA (●) and BAA (○); 1 % starch as substrate in 50 mM Hepes, 20 mM NaCl, pH 7.0 at 20°C.

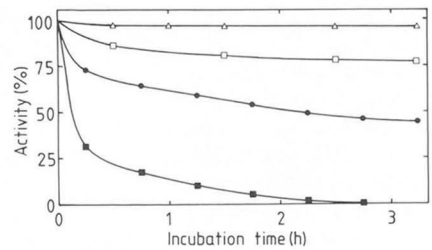

Fig. 3 : Thermal stability of the α-amylases at 45°C. AHA (closed symbols) and BAA (open symbols) were incubated for the indicated periods of time in 50 mM Hepes, pH 7.0 in the presence of 10 mM NaCl (■) or 500 mM NaCl (●) with or without 5 mM $CaCl_2$ (same curves) and 10 mM NaCl (□) or 5 mM $CaCl_2$ (△).

Circular dichroism spectra- The effect of temperature on the secondary structures of the psychrotrophic and the mesophilic enzymes have been studied by far-UV circular dichroism (Fig. 4). AHA displays a mean residue ellipticity Θ at 222 nm of -7,470 ± 150 deg cm² dmol⁻¹ at 25°C, corresponding to an a helix content fα = 17 %. This is a somewhat lower value than the fα = 24 % recorded for BAA in the same conditions and for α-amylases from other *Bacillus* species (23,24). Whereas temperature shift-up from 5 to 55°C induces few alteration of the CD signal of the mesophilic BAA, spectra of AHA are strongly modified at temperatures higher than 40°C, indicating thermal-induced disorganization of the secondary structures (Fig. 4). At the upper experimental temperature, the psychrotrophic enzyme is not completely unfolded as shown by the comparison of the CD spectra recorded in the presence and the absence of 8 M urea (Fig. 4). Figure 5 illustrates the ellipticity variation at 222 nm of both α-amylases as a function of temperature. BAA displays a monotonous ellipticity decrease suggesting that the protein becomes progressively less compact as the temperature increases. The behaviour of AHA is more complex : ellipticity variations are less pronounced in the low temperature range and a sharp denaturation transition occurs at 40°C.

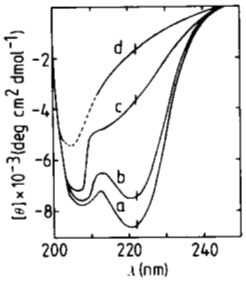

Fig. 4 : Far UV circular dichroism spectra of AHA. Spectra were taken in 25 mM phosphate buffer (pH 7) at 5°C (a), 25°C (b), 55°C (c) and at 25°C in the presence of 8 M urea (d). Protein concentration : 20 µM. Vertical bars indicate the maximal signal oscillation at 222 nm.

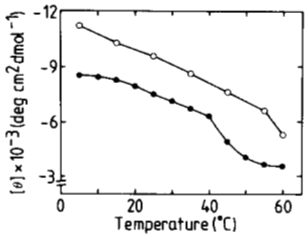

Fig. 5 : Temperature dependence of Θ_{222} of α-amylases. The mean residue ellipticity at 222 nm of AHA (●) 20 µM, mean residue weight of 108.9, and of BAA (○) 13.5 µM, mean residue weight of 113.5, are plotted as a function of the experimental temperature.

Effect of temperature on activity- The thermodependence curves of the amylolytic activity of the psychrotrophic and the mesophilic enzymes are shown in Fig. 6. One can observe the drastic shift towards low temperatures of the apparent optimal temperature of activity of AHA. Also noticeable is the higher k_{cat} (67 s⁻¹) of this enzyme, being 9-fold the value of the mesophilic enzyme at 5°C. The physiological efficiency (k_{cat}/Km) of the cold-adapted enzyme is about 100-fold greater in the temperature range of 5-25°C as a result of its low and stable Km for Et-G_7-PNP (0.2 mM and 2.25 mM at 15°C for AHA and BAA, respectively).

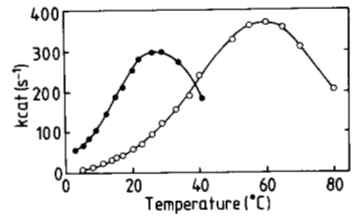

Fig. 6 : Effect of assay temperature on k_{cat} of α-amylases. Amylolytic activity of AHA (●) and BAA (○) were recorded at increasing temperatures using Et-G_7-PNP as substrate.

The above mentioned thermodependence curves have been used to construct Arrhenius plots and to calculate activation energy parameters of the amylolytic reaction. As shown in Table I, both amylases have a comparable ability to reduce the activation energy barrier of the reaction but the contribution of the enthalpy term (ΔH*) and the entropy term (TΔS*) to this free energy of activation (ΔG*) is strikingly different.

TABLE I - Thermodynamic activation parameters for AHA and BAA at 15°C

Parameter	AHA	BAA
k_{cat} (s⁻¹)	187 ± 5 (3)	34 ± 1 (3)
E_a (kJ mol⁻¹)[a]	73 ± 1 (15)	99 ± 2 (12)
ΔG* (kJ mol⁻¹)	58 ± 1	62 ± 2
ΔH* (kJ mol⁻¹)	71 ± 1	97 ± 2
ΔS* (J mol⁻¹ K⁻¹)	46 ± 3	122 ± 6

[a] experimental energy of activation below 15°C

Amino acid sequence determination- 40 N-terminal degradation steps could be achieved on 105 pmol of protein giving rise to 7 % of final yield at the last step. The kinetics of C-terminal amino acid liberation by carboxypeptidase Y is given in Table II. The derived N- and C-terminal amino acid sequences are underlined in figure 7.

TABLE II - Release of COOH-terminal amino acids from purified AHA

incubation time	amino acid released				
	Ser	Ala	Thr	Asx	Leu
min	*mol / mol protein*				
2	0.5				
5	0.8				
10	1.1	0.2			
20	1.3	0.7			
30	1.9	0.8			
60	2.3	0.9	0.4	0.2	
120	2.4	1.0	0.6	0.3	0.2

the deduced carboxyl-terminal sequence is -Leu-Asx-Thr-Ser-Ser-Ala-Ser-COOH

Cloning and sequencing the amy gene- The structural gene of AHA was cloned from a genomic library of *A.haloplanctis* A23. In order to circumvent the thermal denaturation of the cloned gene products, *E.coli* transformants were allowed to grow overnight at 25°C and were then incubated at 0°C for 48 h. Among 30,000 transformants screened by iodine vapours, one clone forming a clear halo of starch hydrolysis was detected. The recombinant plasmid conferring amylolytic activity to *E.coli* was isolated and the AHA gene was sequenced on both strands. The nucleotide sequence, 3,352 bp in length, is shown in figure 7 along with the region coding for the cold active α-amylase and the flanking sequences. Upstream from the ATG codon are short sequences that may function as Shine-Dalgarno translational initiation site and -35, -10 promoters (25). The open reading frame is terminated by a stop codon followed by inverted repeat sequences which may function as transcriptional termination signals. The N-terminal amino acid sequence determination of the native AHA allowed us to locate the signal peptidase cleavage site which fulfils the -3, -1 rule (26). The leader peptide, composed of 24 amino acid residues also follows the general pattern of prokaryotic signal sequences (27). The deduced primary structure of the mature AHA is composed of 453 amino acids with a predicted Mr of 49,340, in good agreement with the electrophoretic estimation. Boxed in figure 7 are the four peptides conserved in all α-amylases. It should be mentioned that removal of the sequence spanning 5' from the first *Hind*III site strongly reduces amylolytic expression in *E.coli*. Such a property suggests the occurrence of a regulatory element, called *amyR* in *Bacillus* (8). This aspect will be discussed elsewhere.